

# We are IntechOpen, the world's leading publisher of Open Access books Built by scientists, for scientists

6,900

Open access books available

186,000

International authors and editors

200M

Downloads

Our authors are among the

154

Countries delivered to

TOP 1%

most cited scientists

12.2%

Contributors from top 500 universities



WEB OF SCIENCE™

Selection of our books indexed in the Book Citation Index  
in Web of Science™ Core Collection (BKCI)

Interested in publishing with us?  
Contact [book.department@intechopen.com](mailto:book.department@intechopen.com)

Numbers displayed above are based on latest data collected.  
For more information visit [www.intechopen.com](http://www.intechopen.com)



# Quantum Computational Chemistry: Modeling and Calculation of S-Block Metal Ion Complexes

*Rakesh Kumar and Sangeeta Obrai*

## Abstract

The computational study of some s-block metal nitrophenolate complexes,  $[\text{Ca}(\text{THEEN})(\text{PIC})]^+$  (**1**),  $[\text{Ca}(\text{THPEN})(\text{H}_2\text{O})_2]^{2+}$  (**2**),  $\text{Ba}(\text{THPEN})(\text{PIC})_2$  (**3**),  $[\text{Na}(\text{THPEN})]_2^{2+}$  (**4**),  $[\text{Sr}(\text{THPEN})(\text{H}_2\text{O})_2]_2^{2+}$  (**5**) and  $[\text{Ba}(\text{THPEN})(\text{H}_2\text{O})_2]_2^{2+}$  (**6**) (where THEEN (N,N,N',N'-Tetrakis(2-hydroxyethyl)ethylenediamine) and THPEN (N,N,N',N'-Tetrakis(2-hydroxypropyl)ethylenediamine) are tetrapodal ligands and  $\text{PIC}^-$  is 2,4,6-trinitrophenolate anion), is presented here using density functional theory (DFT) in its hybrid form B3LYP. The geometries of the title complexes are described by the quantum-chemical approach using input coordinates obtained from the previously synthesized and X-ray characterized diffraction data of  $[\text{Ca}(\text{THEEN})(\text{PIC})](\text{PIC})$ ,  $[\text{Ca}(\text{THPEN})(\text{H}_2\text{O})_2](\text{PIC})_2$ ,  $\text{Ba}(\text{THPEN})(\text{PIC})_2$ ,  $[\text{Na}(\text{THPEN})]_2(\text{PIC})_2$ ,  $[\text{Sr}(\text{THPEN})(\text{H}_2\text{O})_2]_2(\text{DNP})_4$  and  $[\text{Ba}(\text{THPEN})(\text{H}_2\text{O})_2]_2(\text{DNP})_4$  (where DNP is 3,5-dinitrophenolate). Only the primary coordination sphere of complexes (**1–6**) is optimized in the gaseous phase. Calculations of the energy gaps of frontier orbitals (HOMO-LUMO),  $^{13}\text{C}$ -NMR shifts and vibrational bands are carried out using B3LYP/6-31 g + (d,p)/LANL2DZ level of theory. The calculated geometric and spectral parameters reproduced the experimental data with a well agreement.

**Keywords:** DFT, s-block metal complexes, nitrophenolates, tetrapodal ligands

## 1. Introduction

The alkali and alkaline earth metal cations have inert gas electronic structures and are not expected to show any stereochemical requirements in their complex formation as do transition metal cations. They may be considered spherical even in the complex state. Their complexation is thus treated as recognition of spherical cations by organic ligands [1]. Depending upon the nature of the organic ligand and the anion, the metal ions can be separated as solvated ions, solvent separate, loose and tight ion pairs.

Alkali and alkaline earth metal ions form a large number of solid complexes with podands [2–6]. The podands are inherently flexible because the two ends of the molecule are not tied simultaneously. Polypodal ligands are acyclic multidentate ligands containing more than three arms. They form an unlimited family of

structures which finally give rise to dendrimers. A predominant 1:1 complexation has also been observed in alkali and alkaline earth metal complexes of the tetra- and pentapodands. The stability constants of the tetrapodands are generally lower than those of the corresponding tripodands because of more severe steric hindrance to complexation [7]. Vögtle and coworkers have indicated that the ligands resembling tetrapodands are capable of forming 1:1 complexes with s-block metal ions [8, 9].

The s-block elements present a usual challenge in the molecular modeling, because the metal-ligand interactions in both cases are principally electrostatic. The types of alkali and alkaline earth metal complexes subjected to molecular modeling can be divided into five categories: crown ethers [10–16], cryptands [17, 18], spherands [19, 20], podands and other biologically important ligands, such as ionophores and cyclic antibiotics [21–24]. The present work has been undertaken with the aim to computationally characterize the structure and nature of complexes of s-block metal ions with the tetrapodands THEEN and THPEN. Recently the computational studies of these tetrapodal ligands with Cu(II), Ag(I) and La(III) have been reported. Recently, synthesis, crystal structure and biological properties of  $[\text{Co}(\text{edtp})\text{Cl}]\cdot\text{NO}_3\cdot\text{H}_2\text{O}$  complex was also determined, where edtp is N,N,N',N'-Tetrakis(2-hydroxypropyl) ethylenediamine in which  $\text{Co}^{2+}$  ion is coordinated by the N,N',O,O'-pentadentate edtp ligand and a chloride to generate a distorted  $\text{CoClN}_2\text{O}_3$  octahedron [25–28].

## 2. Computational details

From the last 3 decades density functional theory has been the dominant method for the quantum mechanical simulation of periodic systems. In recent years it has also been adopted by quantum chemists and is now very widely used for the simulation of energy surfaces in molecules. The quantum-chemical calculations (DFT calculations) giving molecular geometries of minimum energies, molecular orbitals (HOMO-LUMO),  $^{13}\text{C}$ -NMR and vibrational spectra were performed using the Gaussian 09 [29]. Molecular orbitals were visualized using “Gauss view”. The method used was Becke’s three-parameter hybrid-exchange functional, the nonlocal correlation provided by the Lee, Yang and Parr expression, and the Vosko, Wilk, and Nuair 1980 local correlation functional (III) (B3LYP) [30, 31]. The 6-31 g + (d,p) basis set was used for C, N and O. The LANL2DZ basis set [32] and pseudopotentials of Hay and Wadt were used for Ca, Sr, Ba and Na metal atoms [33, 34]. DFT calculations were performed in the gaseous phase and the input coordinates were obtained from and then compared with crystal structure data of already reported complexes:  $[\text{Ca}(\text{THEEN})(\text{PIC})](\text{PIC})$ ,  $[\text{Ca}(\text{THPEN})(\text{H}_2\text{O})_2](\text{PIC})_2$ ,  $\text{Ba}(\text{THPEN})(\text{PIC})_2$ ,  $[\text{Na}(\text{THPEN})]_2(\text{PIC})_2$ ,  $[\text{Sr}(\text{THPEN})(\text{H}_2\text{O})_2]_2(\text{DNP})_4$  and  $[\text{Ba}(\text{THPEN})(\text{H}_2\text{O})_2]_2(\text{DNP})_4$  (where DNP is 3,5-dinitrophenolate) [35]. The structural parameters were adjusted until an optimal agreement between calculated and experimental structure obtained throughout the entire range of available structures. HOMO-LUMO analyses and spectroscopic calculations were performed on the optimized geometries of the title complexes (1–6) using B3LYP/6-31 g + (d,p)/LANL2DZ level of theory.

## 3. Geometrical structures

### 3.1 Results and discussion

Complexes (1–6) were successfully modeled by using the input coordinates of crystal data. **Tables 1** and **2** represent comparison of calculated and experimental

	Complex 1 (M = Ca)			Complex 2 (M = Ca)			Complex 3 (M = Ba)		
	Theo.	Exp.	Dev.	Theo.	Exp.	Dev.	Theo.	Exp.	Dev.
M-O1	2.450	2.410	0.040	2.389	2.341	0.048	2.720	2.722	-0.002
M-O2	2.450	2.380	0.070	2.495	2.498	-0.003	2.807	2.812	-0.006
M-O3	2.410	2.480	0.070				2.753	2.753	0.000
M-O4	2.410	2.370	0.040				2.812	2.816	-0.004
M-O5							2.681	2.687	-0.006
M-O6							3.127	3.135	-0.008
M-O12	2.310	2.30	0.01				2.728	2.735	-0.007
M-O13	2.470	2.73	0.26						
M-O18							2.977	2.990	-0.013
M-O1W				2.440	2.442	-0.002			
M-O2W									
M-N1	2.824	2.591	0.233	2.601	2.603	-0.002	3.038	3.042	0.004
M-N2	2.738	2.658	0.08				3.026	3.032	-0.006

**Table 1.**  
 Comparison of experimental and calculated M-ligand bond lengths (Å) of complexes (1–3).

	Complex 4 (M = Na)			Complex 5 (M = Sr)			Complex 6 (M = Ba)		
	Theo.	Exp.	Dev.	Theo.	Exp.	Dev.	Theo.	Exp.	Dev.
M-O1	2.412	2.416	-0.004	2.617	2.628	-0.011	2.736	2.743	-0.007
M-O2	2.393	2.396	-0.003	2.611	2.618	-0.007	2.763	2.767	-0.004
M-O3	2.505	2.508	-0.003	2.506	2.516	-0.010	2.756	2.762	-0.006
M-O4	2.628	2.632	-0.004	2.618	2.626	-0.008	2.658	2.668	-0.010
M-O1W				2.701	2.711	-0.010	2.880	2.884	-0.004
M-O2W				2.699	2.705	-0.006	2.988	2.995	-0.007
M-O2WA				2.726	2.732	-0.006			
M-N1				2.835	2.842	-0.007	3.009	3.008	-0.001
M-N2				2.849	2.857	-0.008	3.010	3.010	0.000

**Table 2.**  
 Comparison of experimental and calculated M-ligand bond lengths (Å) of complexes (4–6).

M-Ligand bond lengths (Å) of complexes (1–3) and (4–6), respectively. The picrates and dinitrophenolates that are excluded from the primary coordination spheres of metal atoms in the crystallographic determinations, are not optimized in the computed structures. **Tables 3** and **4** represent comparison of calculated and experimental torsion angles of ligand in complexes (1–3) and (4–6) respectively.

### 3.1.1 [Ca(THEEN)(PIC)]<sup>+</sup> (1)

The coordination number of Ca(II) ion is eight with distorted cube geometry in the optimized geometry of cationic complex (1) (**Figure 1**). THEEN is interacting with Ca(II) ion through all the six potential donor atoms. The seventh and eighth coordination sites of Ca(II) are occupied by picrate anion through phenolic oxygen

Name of the Atoms	Complex (1)			Complex (2)			Complex (3)		
	Theo.	Exp.	Dev.	Theo.	Exp.	Dev.	Theo.	Exp.	Dev.
O1-C1-C2-N1	-55.1	-55.05	0.05	57.9	58.0	0.1	-32.3	-32.4	-0.1
C1-C2-N1-C5	165.1	165.1	0.0	82.8	82.7	0.1	161.9	162.0	0.1
C2-N1-C5-C6	-159.0	-159.0	0.0	-165.5	-165.5	0.0	-157.6	-157.8	-0.2
N1-C5-C6-N2	65.4	65.3	0.1	60.4	60.5	0.1	65.9	66.1	0.2
C5-C6-N2-C8				-159.1	-159.0	0.1	-159.3	-159.4	0.1
C6-N2-C8-C7				89.1	89.1	0.0	163.6	163.7	0.1
N2-C8-C7-O3				60.9	60.9	0.0	-34.1	-34.2	-0.1
O2-C3-C4-N1	36.5	36.7	0.2	55.5	55.6	0.1	46.8	46.9	-0.1
C3-C4-N1-C5	-121.6	-121.7	-0.1	-161.0	-161.0	0.0	-132.6	-132.7	-0.1
C4-N1-C5-C6	77.2	77.2	0.0	72.6	72.6	0.0	83.7	83.8	0.1
C5-C6-N2-C10				79.4	79.4	0.0	79.0	79.1	0.1
C6-N2-C10-C9				-151.8	-151.8	0.0	-134.9	-134.9	0.0
N2-C10-C9-O4				61.3	61.4	0.1	52.1	52.2	0.1

**Table 3.**

Comparison of calculated and experimental torsion angles ( $^{\circ}$ ) of ligand in the complexes (1–3).

Name of the Atoms	Complex (4)			Complex (5)			Complex (6)		
	Theo.	Exp.	Dev.	Theo.	Exp.	Dev.	Theo.	Exp.	Dev.
Complex	-55.6	-55.7	-0.1	32.3	32.3	0.0	-43.4	-43.5	0.1
O1-C1-C2-N1	152.7	152.6	0.1	-143.9	-143.9	0.0	162.3	162.4	0.1
C1-C2-N1-C5	-80.2	-80.2	0.0	86.1	86.1	0.0	-92.7	-92.8	0.1
C2-N1-C5-C6	-64.0	-63.9	-0.1	43.6	43.6	0.0	-50.1	-50.1	0.0
N1-C5-C6-N2	165.5	165.4	0.1	-146.4	-146.4	0.0	156.5	156.7	0.2
C5-C6-N2-C8	-85.7	-85.7	0.0	156	155.9	0.1	-89.6	-89.9	0.3
C6-N2-C8-C7	-60.3	-60.4	-0.1	-44.7	-44.7	0.0	-30.4	-30.4	0.0
N2-C8-C7-O3	-59.7	-59.8	-0.1	-17.4	-17.4	0.0	47.8	48.1	0.3
O2-C3-C4-N1	-91.0	-91.1	-0.1	112.7	112.7	0.0	-135.1	-135.2	0.1
C3-C4-N1-C5	156.0	156.0	0.0	-159.1	-159.2	0.1	151.9	151.9	0.0
C4-N1-C5-C6	-72.4	-72.5	-0.1	97.4	97.4	0.0	-92.1	-92.4	0.3
C5-C6-N2-C10	156.6	156.6	0.0	-151.8	-151.8	0.0	143.4	143.9	0.5
C6-N2-C10-C9	-59.2	-59.3	-0.1	41.6	41.7	0.1	5.1	4.9	0.3
N2-C10-C9-O4	-55.6	-55.7	-0.1	32.3	32.3	0.0	-43.4	-43.5	0.1

**Table 4.**

Comparison of experimental and calculated and torsion angles ( $^{\circ}$ ) of ligand in the complexes (4–6).

and one of the o-nitro oxygen. The observed and calculated positions of calcium and donor atoms are in agreement. A comparison of bond lengths and bond angles provided a maximum tolerance of 0.27 Å and 16.33° Å, respectively (**Table 1** and **Table S1; Figure S1a,b**) of computed title complex (1) and crystallographically determined complex [Ca(THEEN)(PIC)](PIC). The torsion angles of the ligand THEEN in theoretically determined and experimental complex are also in well

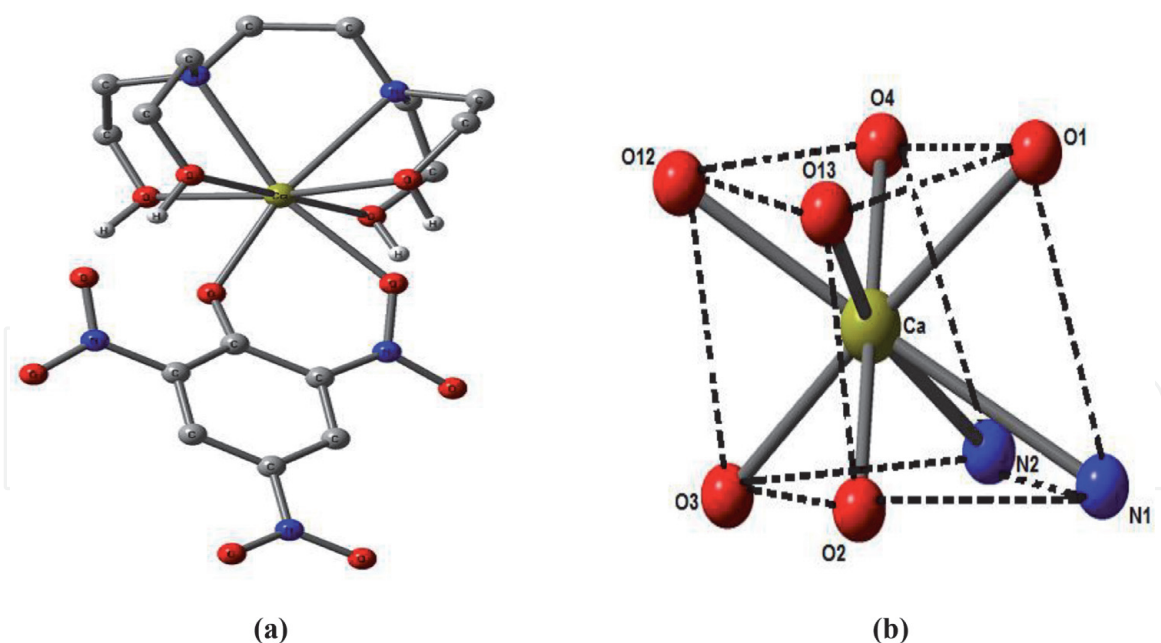


**Figure 1.**

(a) Optimized geometric structure of  $[Ca(THPEN)(PIC)]^+$  (1) (b) distorted cube geometry.

consistency with each other (**Table 3**). The HOMO-LUMO analysis has indicated that there is maximum distribution of HOMO over the carbon atoms and to a lesser extent on the oxygen of the coordinated picrate. LUMO is mainly distributed or concentrated on all the atoms of coordinated picrate except p-nitro group. Neither HOMO nor LUMO distribution is found either on calcium ion or on any ligand atom. The HOMO-LUMO gap ( $\Delta E$ ) is found to be 0.852 eV (**Figure S1c**).

### 3.1.2 $[Ca(THPEN)(H_2O)_2]^{2+}$ (2)

Ca(II) is eight coordinated in monomeric cationic complex with a distorted square-antiprismatic geometry in complex (2) as is observed in crystal structure of  $[Ca(THPEN)(H_2O)_2](PIC)_2 \cdot H_2O$  (**Figure 2**). THPEN is acting as hexadentate ligand towards the metal ion. Two remaining sites around the metal ion are occupied by two water molecules. The observed and calculated positions of calcium and donor atoms are in agreement. All strain energy minimized structures reproduced the observed X-ray structures with almost no deviation in M-L bond length and torsion angle of the ligand (**Table 3**). The maximum tolerance of L-M-L bond angle is 15.8° (**Tables 1 and Table S1, Figure S2a,b**). Complex 2 is displaying the main distribution of HOMO as well as LUMO only on water molecules. There is slight distribution of HOMO and LUMO on hydroxyl oxygen of THPEN ligand also with HOMO-LUMO gap (HLG) of 0.419 eV (**Figure S2c**).

### 3.1.3 $Ba(THPEN)(PIC)_2$ (3)

Ba(II) is ten-coordinate in its monomeric complex (3) (**Figure 3**). The ligand THPEN coordinates through both its nitrogen atoms and all the four hydroxyl oxygen. The two picrate ions are also directly coordinated to  $Ba^{2+}$  ion through the phenolic oxygen and one oxygen of the o-nitro group. Since both the picrates are directly interacting with the cation, the complex is termed as tight ion-paired complex as is found in the crystallographically determined complex. The observed and calculated positions of barium and donor atoms are in agreement. There is negligible deviation found in bond length, bond angle (0.11°) and torsion angle of ligand THPEN for calculated title complex (3) and experimental  $Ba(THPEN)(PIC)_2$

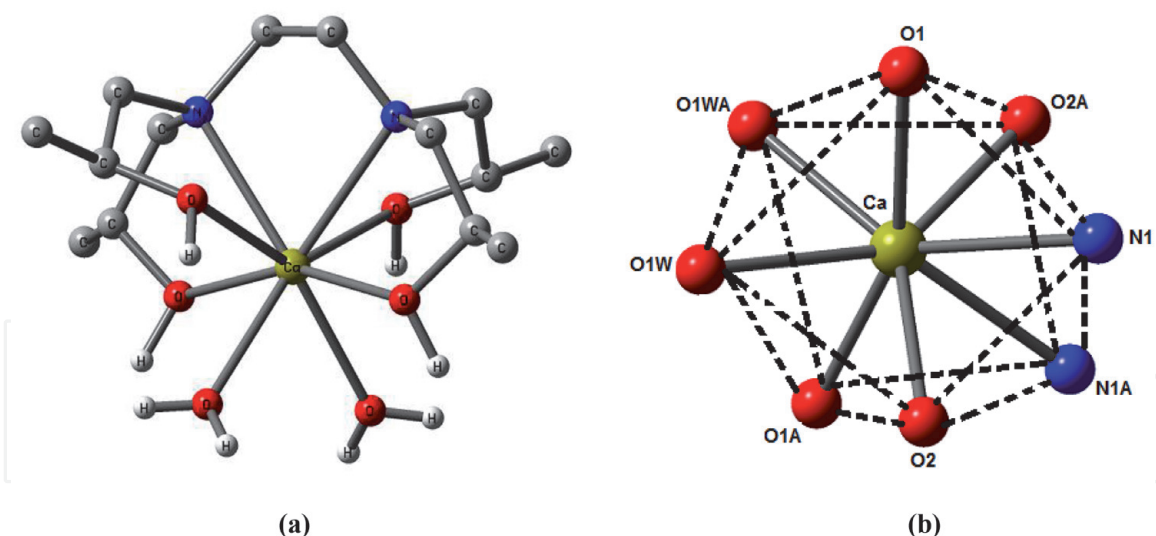


**Figure 2.**  
 (a) Optimized geometric structure of  $[Ca(THPEN)(H_2O)_2]^{2+}$  (2) (b) distorted square-antiprismatic geometry.

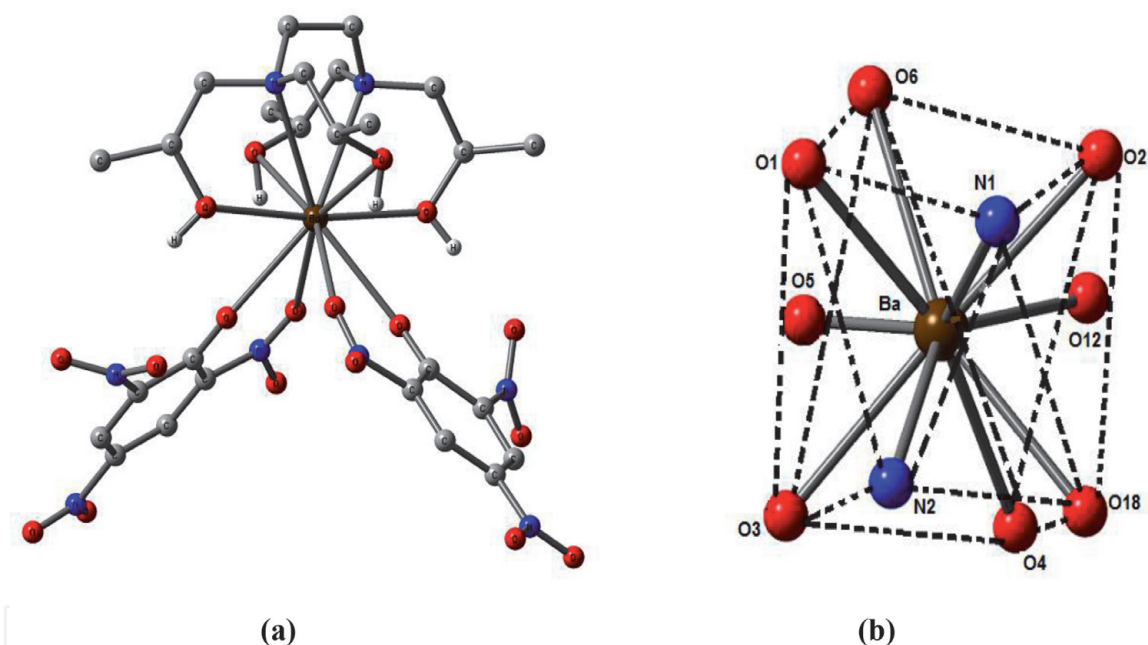


**Figure 3.**  
 (a) Optimized geometric structure of  $Ba(THPEN)(PIC)_2$  (3) (b) bicapped square-antiprismatic geometry.

(Tables 1 and 3 and S1, Figure S3a,b). An analysis of HOMO-LUMO has illustrated that HOMO is mainly distributed on the ligand THPEN with a small distribution on coordinated picrates. In contrast to this LUMO is mainly distributed on coordinated picrates with no distribution over the ligand or metal atom. The complex is showing HLG of 0.118 eV (Figure S3c).

### 3.1.4 $[Na(THPEN)]_2^{2+}$ (4)

**Figure 4a** shows the optimized structure of the cationic complex of sodium (4). This structure is centrosymmetric dimer. The coordination number around each  $Na^+$  ion is seven. Each THPEN ligand coordinates to  $Na(I)$  ion in a heptadentate fashion (**Figure 4**). In other words, one hydroxyl group of the THPEN ligand acts as a bridge between two  $Na^+$  ions. The geometry of the complex is distorted monocapped octahedron. The Na ... Na non bridging distance is 3.429 Å. Almost no

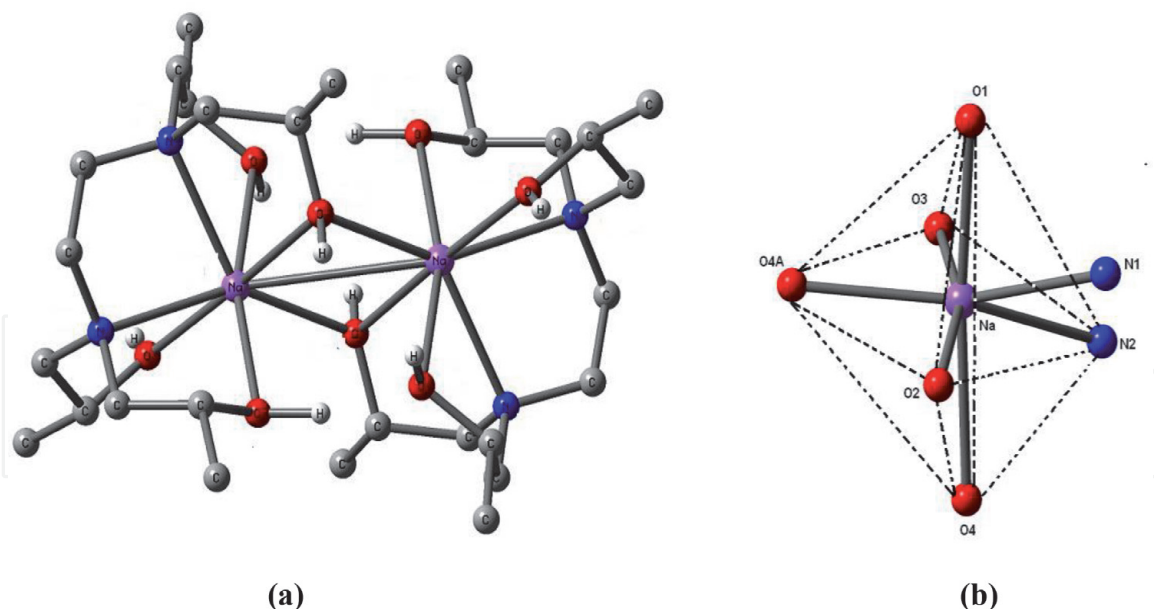


**Figure 4.**  
(a) Optimized geometric structure of  $[Na(THPEN)]_2^{2+}$  (4) (b) distorted monocapped octahedron geometry.

deviation has been observed in bond length (M-L), torsion angle of ligand THPEN and bond angles (L-M-L) of computed title complex (4) and crystallographically determined complex  $[Na(THPEN)]_2(PIC)_2$  (Tables 2 and 4 and Table S1, Figures S4a,b). The HOMO-LUMO study has revealed that in the title complex (4) HOMO is mainly concentrated on bridged hydroxyl oxygens and sodium metal but to a smaller extent on the other coordinated hydroxyl oxygens and amine nitrogens. LUMO is mainly concentrated on bridged hydroxyl oxygens and to a smaller extent on other coordinated oxygen atoms. The HOMO-LUMO gap is 0.261 eV (Figure S4c).

### 3.1.5 $[Sr(THPEN)(H_2O)_2]_2^{2+}$ (5)

Sr(II) is nine-coordinated in its dimeric complex (5) (Figure 5). This cationic complex is having tricapped trigonal-prismatic geometry as is found in crystallographically determined complex  $[Sr(THPEN)(H_2O)_2]_2(DNP)_4$ . Each  $Sr^{2+}$  ion in the complex is coordinated by six potential donor sites of the ligand THPEN and four water molecules. Out of four water molecules, two are bridging and the third one is non-bridging. Sr...Sr non bridging distance is 4.346 Å indicating the existence of van der Waals contact. All strain energy minimized structures reproduced the observed X-ray structures to a maximum tolerance of 9.07° bond angle (Table 2 and Table S1, Figure S5a,b). Almost no deviation of M-L bond length and torsion angle of ligand THPEN has been observed for the title complex (5) and crystallographically determined complex (Tables 2 and 4). The HOMO-LUMO analysis has shown that the complex (5) is having maximum distribution of HOMO and LUMO on bridged coordinated water molecules and there is HLG of 0.0225 eV (Figure S5c).

### 3.1.6 $[Ba(THPEN)(H_2O)_2]_2^{2+}$ (6)

Ba(II) is ten-coordinate in the cationic title complex (6) as is found in the crystallographic determined complex  $[Ba(THPEN)(H_2O)_2]_2(DNP)_4$ . The geometry around Ba(II) is bicapped cubic. Each Ba(II) in dimer is interacting with THPEN through all its six potential donor sites and four water molecules. The latter are

bridging in nature. The existence of van der Waals contact between non-bridging Ba ... Ba is indicated by their larger distance (4.196 Å). The observed and calculated positions of the metal and donor atoms are in agreement as almost negligible deviation of M-L bond length and torsion angle of THPEN. A deviation of 0.14° of bond angle L-M-L has been observed for complex (6) [Ba(THPEN)(H<sub>2</sub>O)<sub>2</sub>](DNP)<sub>4</sub> (Tables 2 and 4 and Table S1; Figures S6a,b and S7). The region of distribution of HOMO and LUMO is only over two of the bridged water molecules in complex (6) with a very small HOMO-LUMO gap ( $\Delta E = 0.0375$  eV) indicating the soft nature of complex (Figure 6).

### 3.2 HOMO-LUMO analyses

Smaller is the HUMO-LUMO gap (HLG) softer is the complex [36, 37]. The frontier orbitals HOMO and LUMO are very important parameters for chemical reaction and take part in chemical stability [38–40]. It is predicted from the HOMO-LUMO gaps that the title complexes are soft as is obvious from their smaller HUMO-LUMO energy gaps (HLG) relative to the similar reported complexes of

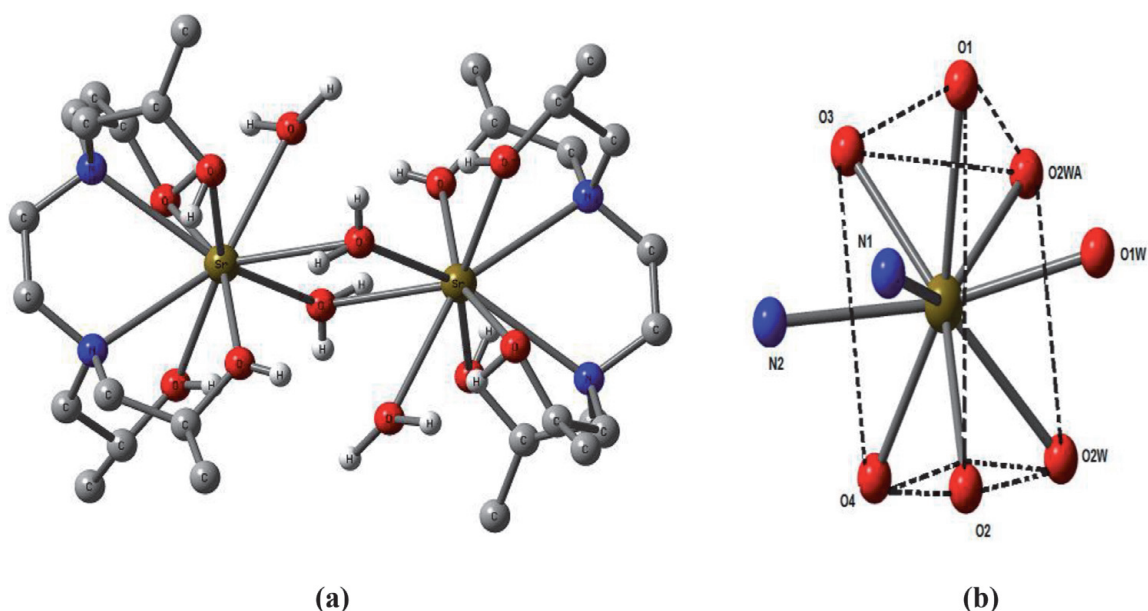


**Figure 5.** (a) Optimized geometric structure of [Sr(THPEN)(H<sub>2</sub>O)<sub>2</sub>]<sub>2</sub>(DNP)<sub>4</sub> (b) Trigonal- prismatic geometry.

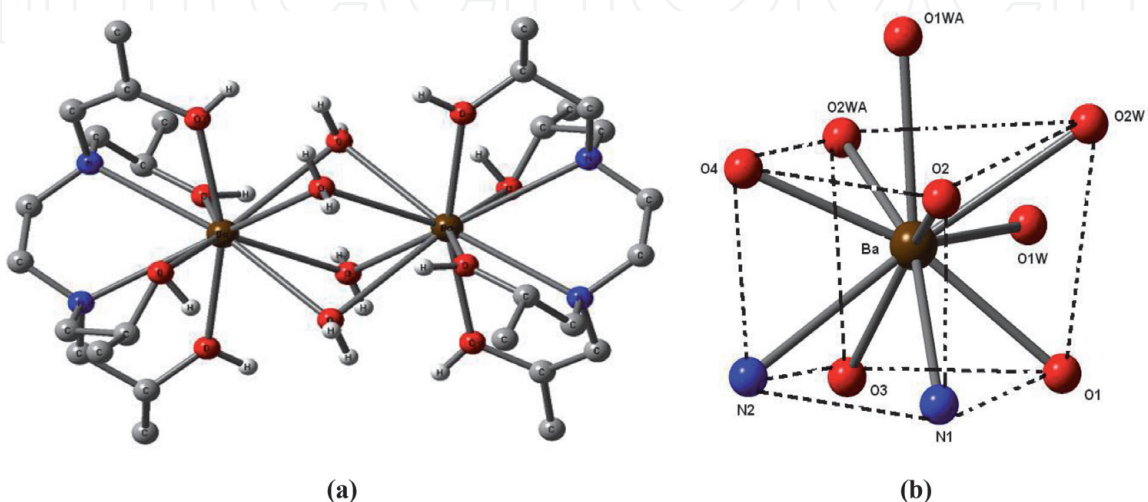


**Figure 6.** (a) Optimized geometric structure of [Ba(THPEN)(H<sub>2</sub>O)<sub>2</sub>]<sub>2</sub><sup>2+</sup> (6) (b) Bicapped cubic geometry.

copper, silver and lanthanoid [25–27] (Table 5). It has been observed in the present computational study that the dinitrophenolate complexes are softer than trinitrophenolate and among the latter, [Ca(THEEN)(PIC)]<sup>+</sup> (1) is displaying least softness. It is pertinent to mention here that the complex (1) is having THEEN ligand whereas THPEN is ligand in rest of the complexes (2–6).

### 3.3 Spectral data

Nuclear magnetic resonance spectra (NMR) and infrared (IR) spectroscopy can be useful for studying the coordination of various ligating sites. The <sup>13</sup>C-NMR spectra were predicted for complexes (1–6) using DFT/B3LYP/6-31G\*\* method and the spectral data was compared with experimental data reported in literature [35]. The computed NMR spectral data is fairly in agreement with experimental data (Tables 6 and 7). Small deviations are due to the fact that H-bonding interactions or any type of lattice interactions are not modeled in theoretically computed structures. The terminal methyl groups in theoretically predicted complexes (2–5) are

	HLG (eV)	Reported complexes	HLG (eV)	Reported complexes	HLG (eV)
[Ca(THEEN)(PIC)] <sup>+</sup> (1)	0.852	[Cu(THEEN)(H <sub>2</sub> O)] <sub>2</sub> (PIC) <sub>2</sub>	3.537	[La(THEEN)(PIC)(H <sub>2</sub> O) <sub>2</sub> ] <sub>2</sub> (PIC) <sub>2</sub> .2H <sub>2</sub> O	3.428
[Ca(THPEN)(H <sub>2</sub> O) <sub>2</sub> ] <sup>2+</sup> (2)	0.419	[Cu(THPEN)] <sub>2</sub> (PIC) <sub>2</sub> .C <sub>3</sub> H <sub>8</sub> O	3.467	[La(TEAH <sub>3</sub> )(H <sub>2</sub> O) <sub>2</sub> ] <sub>2</sub> (PIC) <sub>3</sub>	3.673
Ba(THPEN)(PIC) <sub>2</sub> (3)	0.118	[Cu(TEAH <sub>3</sub> )(PIC)] <sub>2</sub> (PIC).H <sub>2</sub> O	3.619		
[Na(THPEN)] <sub>2</sub> <sup>2+</sup> (4)	0.261	[Ag(THEEN)] <sub>2</sub> (PIC) <sub>2</sub>	2.530		
[Sr(THPEN)(H <sub>2</sub> O) <sub>2</sub> ] <sup>2+</sup> (5)	0.0225	[Ag(THPEN)] <sub>2</sub> (PIC) <sub>2</sub>	2.640		
[Ba(THPEN)(H <sub>2</sub> O) <sub>2</sub> ] <sup>2+</sup> (6)	0.0375	[Ag(TEAH <sub>3</sub> ) <sub>2</sub> ](PIC)	1.061		

**Table 5.** Comparison of HOMO-LUMO energy gaps of complexes (1–6) with earlier reported complexes [25–27].

Assignments (δ)	[Ca(THEEN)(PIC)] <sup>+</sup> (1)		Ba(THPEN)(PIC) <sub>2</sub> (3)	
	Theo.	Exp.	Theo.	Exp.
—CH <sub>3</sub>	*	*	4.22	19.61
—CH <sub>3</sub>			4.49	19.89
—NCH <sub>2</sub>	52.31	55.03	51.73	55.34
—NCH <sub>2</sub>			43.35	55.20
—OCH <sub>2</sub> , —OCH	59.03	57.47	50.75	63.00
—ArCH	113.63	124.33	117.85	124.36
p-ArCN	134.75	123.60	122.06	123.68
o-ArCN	140.68	140.78	140.98	140.78
—ArCO	161.57	160.20	150.21	160.20

\* Group absent.

**Table 6.** Comparison of calculated and experimental <sup>13</sup>C-NMR spectral data for complexes (1 and 3).

Assignment ( $\delta$ )	[Ca(THPEN)(H <sub>2</sub> O) <sub>2</sub> ] <sup>2+</sup> (2)		[Na(THPEN)] <sub>2</sub> <sup>2+</sup> (4)		[Sr(THPEN)(H <sub>2</sub> O) <sub>2</sub> ] <sup>2+</sup> (5)		[Ba(THPEN)(H <sub>2</sub> O) <sub>2</sub> ] <sup>2+</sup> (6)	
	Theo.	Exp.	Theo.	Exp.	Theo.	Exp.	Theo.	Exp.
—CH <sub>3</sub>	11.35	18.79	4.01	20.30	3.77	18.31	27.02	18.35
—CH <sub>3</sub>	11.38	19.02	5.63	20.36	3.85	18.59	27.69	18.63
—NCH <sub>2</sub>	39.60	50.99	43.05	50.42	43.60	48.31	61.69	59.80
—NCH <sub>2</sub>	39.61	51.76	44.05	52.90	57.81	59.68	61.69	60.59
—OCH	*	*	50.73	55.73	41.85	60.62	60.37	60.66
—OCH	69.24	61.74	57.90	55.95	51.91	61.08	60.38	62.53

\* Group absent.

**Table 7.**  
Comparison of calculated and experimental <sup>13</sup>C-NMR spectral data for complexes (2, 4–6).

Assignments (cm <sup>-1</sup> )	[Ca(THEEN)(PIC)] <sup>+</sup> (1)		[Ca(THPEN)(H <sub>2</sub> O) <sub>2</sub> ] <sup>2+</sup> (2)		Ba(THPEN)(PIC) <sub>2</sub> (3)	
	Theo.	Exp.	Theo.	Exp.	Theo.	Exp.
$\nu$ (NO <sub>2</sub> )	1363.56	1360 m	1320.81	1360 vs	1384.20	1370
$\delta$ (=CH)	696.80	700 m	784.16	790 m	800	800

**Table 8.**  
Comparison of calculated and experimental IR spectral data for complexes (1–3).

Assignments (cm <sup>-1</sup> )	[Na(THPEN)] <sub>2</sub> <sup>2+</sup> (4)		[Sr(THPEN)(H <sub>2</sub> O) <sub>2</sub> ] <sup>2+</sup> (5)		[Ba(THPEN)(H <sub>2</sub> O) <sub>2</sub> ] <sup>2+</sup> (6)	
	Theo.	Exp.	Theo.	Exp.	Theo.	Exp.
$\nu$ (NO <sub>2</sub> )	1366	1371.21	1330	1329.24	1340	1329.43
$\delta$ (=CH)	790	784.54	760	762.52	790	787.17

**Table 9.**  
Comparison of calculated and experimental IR spectral data for complexes (4–6).

displaying quiet high upfield shifts relative to the experimentally obtained due to more free movements in the gaseous phase than in solution or solid phase.

The computed IR spectral peaks that appear in the range of 1370–600 cm<sup>-1</sup> are fairly in agreement with the experimental data (Tables 8 and 9). The absorption peaks due to the presence of hydroxyl groups were observed only for complexes (1) and (6) in the computed IR spectra. It is pertinent to mention here that both of these complexes possess the picrate anion in their coordination sphere. The less extent of H-bonding is reported in the crystallographic description of these complexes [35]. The theoretical absorption band appears at 3223 and 3235 cm<sup>-1</sup> for both complexes (1) and (6) whereas the experimental band is reported at 3300 cm<sup>-1</sup> for both of them [35].

## 4. Conclusions

The coordination number of the title s-block complexes is varying from 7 to 10 in the present work. As the size of the metal increases, coordination number of

central metal ion also increases. Out of the six complexes presented, three are monomeric (1–3) and three are dimeric (4–6). The longer distances between two M...M distances in the dinuclear complexes indicate the existence of van der Waals contacts between the two s-block metal ions. All the title complexes are cationic except Ba(THPEN)(PIC)<sub>2</sub> (3). The latter is tight ion-paired complex. All strain energy minimized structures obtained using quantum-chemical approach reproduced the observed X-ray structures with geometric parameters in well agreement. HOMO-LUMO studies suggest the softness of the title s-block complexes relative to the similar already reported copper, silver and lanthanoid complexes. The theoretical spectral data (<sup>13</sup>C-NMR and IR) computed using DFT and experimental data is fairly in agreement with each other. The accuracy of the results predicts that the DFT studies performed using B3LYP/6-31 g + (d,p)/LANL2DZ level of theory is the appropriate quantum-chemical method for reproducing the experimental results for the title s-block complexes. This quantum-chemical approach has potential for molecular modeling of other s-block complexes and exploring their chemistry.

Small deviations in geometric as well as spectral parameters may be attributed to the lack of H-bonding and packing interactions within lattice which were not modeled during the computational study of the entitled s-block complexes. Moreover, the quantum-chemical approach of DFT studies has been carried out in the gaseous phase whereas the already reported experimental crystal and IR spectral data is in the solid phase while <sup>13</sup>C-NMR spectral data is in the solution phase.

## Appendix

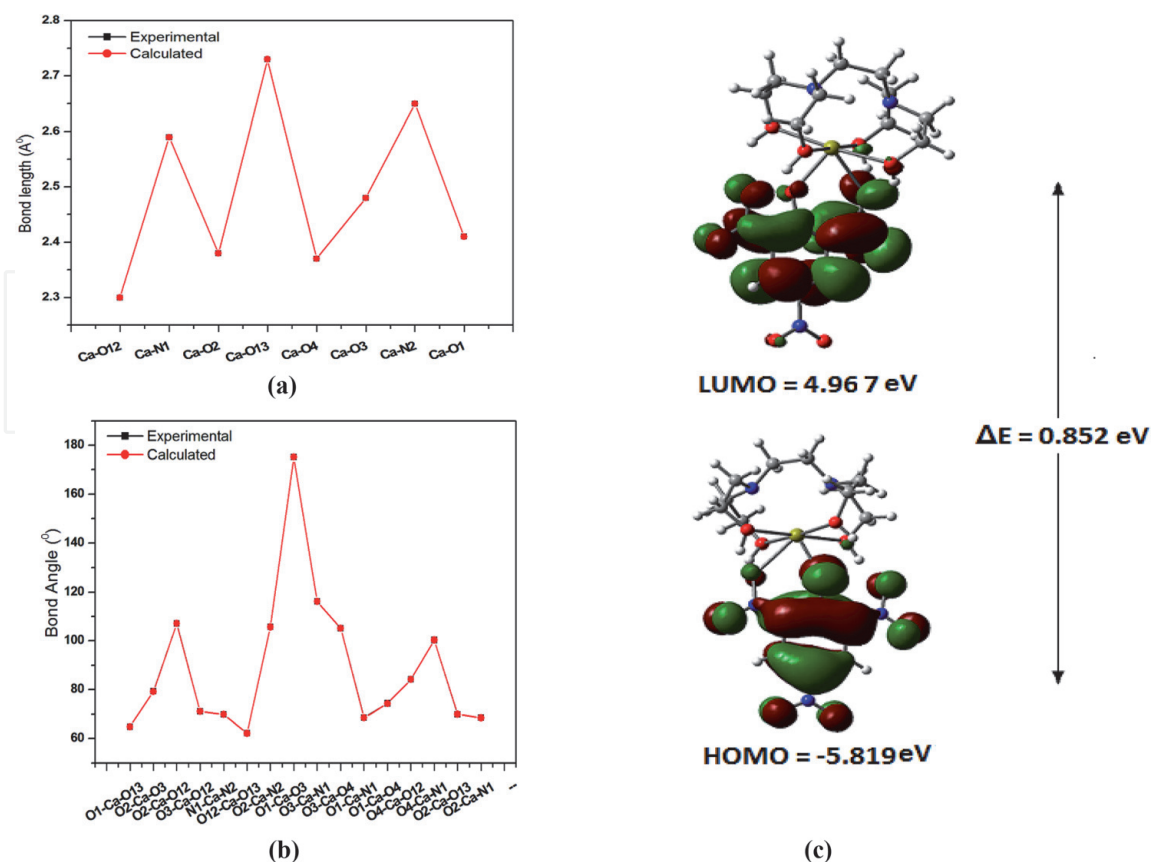
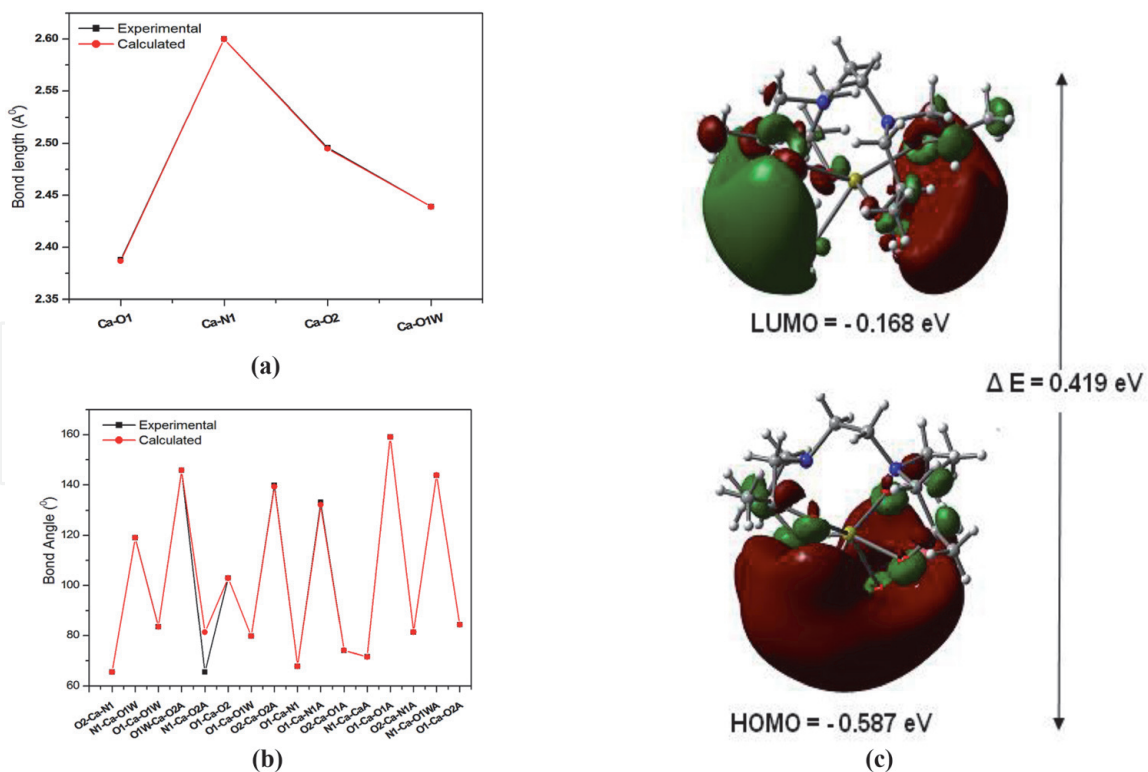


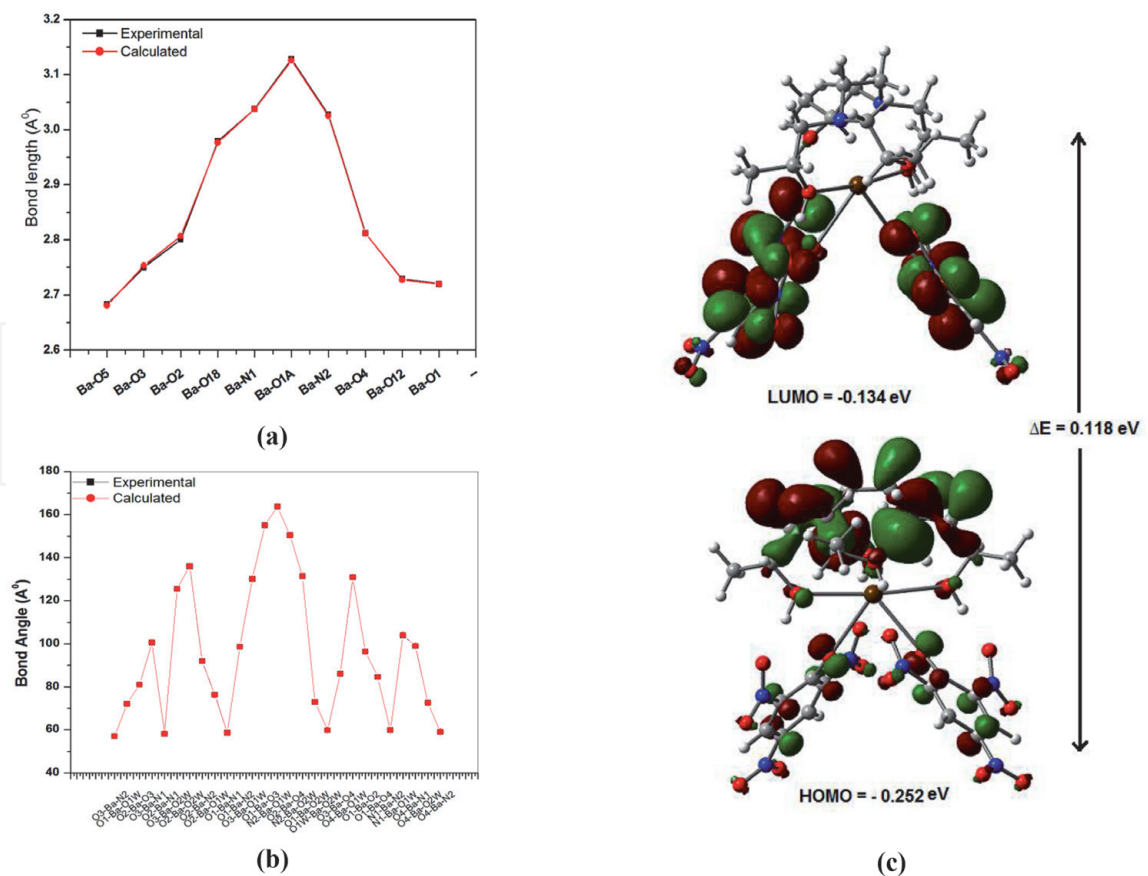
Figure S1.

Plot showing the deviations of theoretical and experimental (a) bond lengths (Å) and (b) bond angles (°) for the complex (1) and (c) (HOMO-LUMO) of the complex (1) with energy gap.



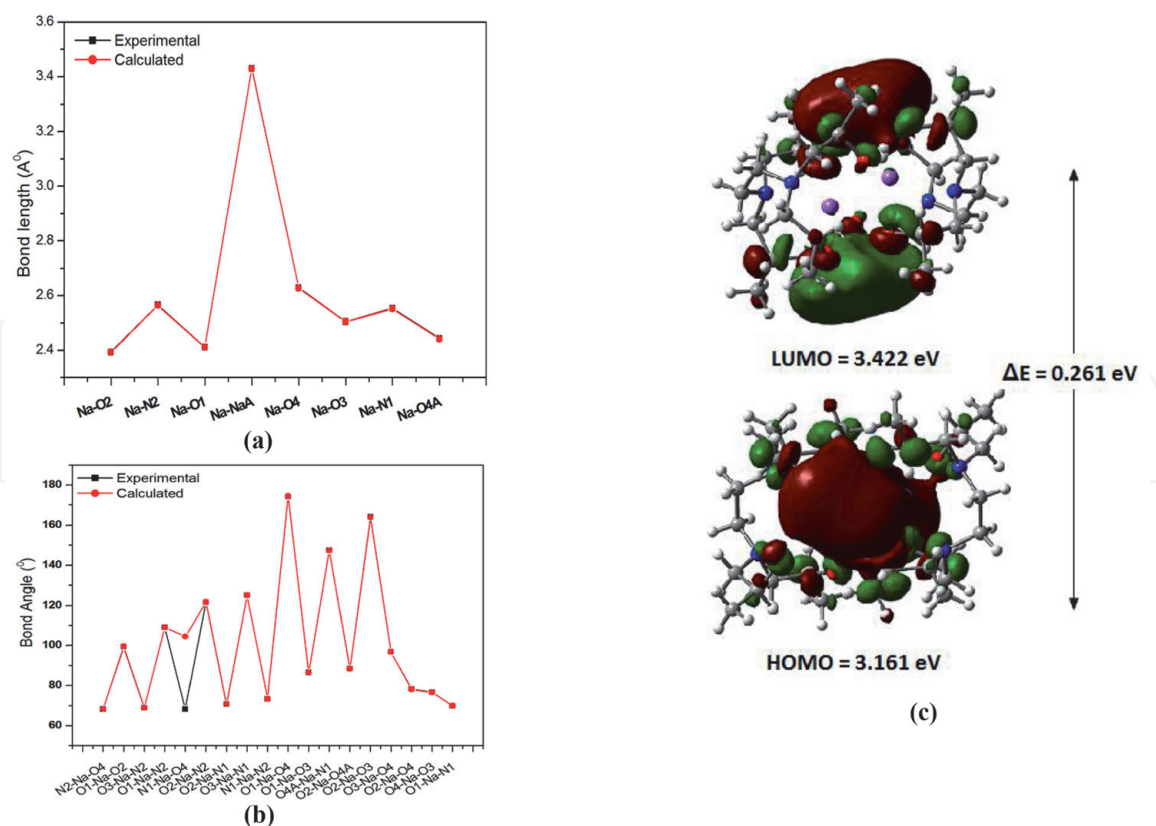
**Figure S2.**

Plot showing the deviations of theoretical and experimental (a) bond lengths ( $\text{\AA}$ ) and (b) bond angles ( $^\circ$ ) for the complex (2) (c) (HOMO-LUMO) of the complex (2) with energy gap.

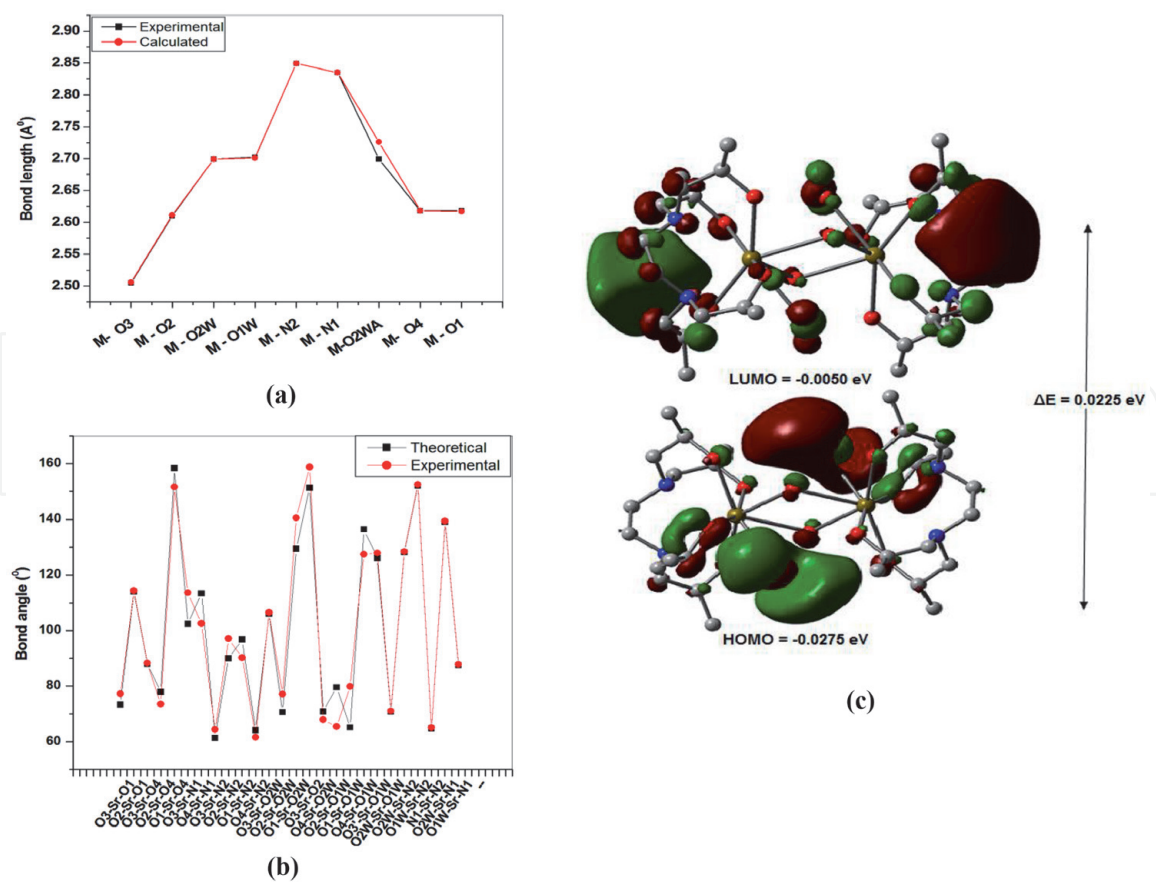


**Figure S3.**

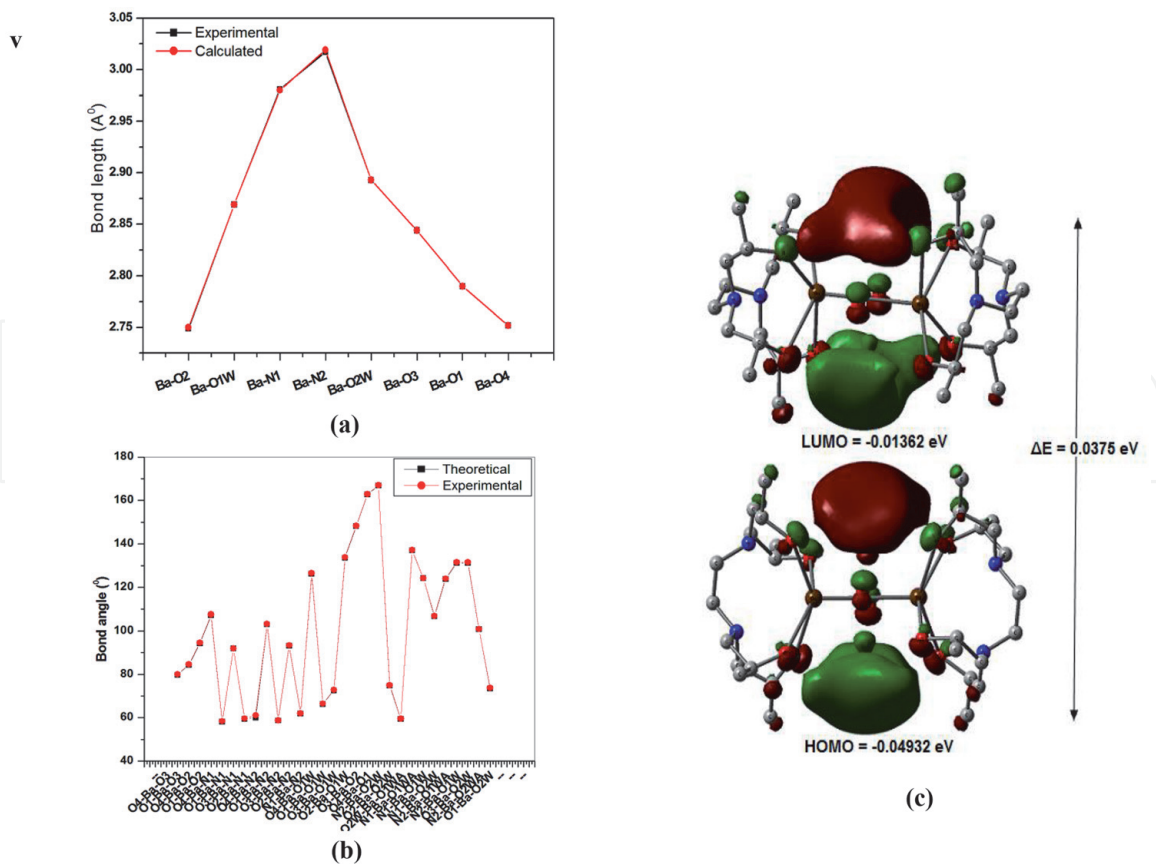
Plot showing the deviations of theoretical and experimental (a) bond lengths ( $\text{\AA}$ ) and (b) bond angles ( $^\circ$ ) for the complex (3) (c) (HOMO-LUMO) of the complex (3) with energy gap.



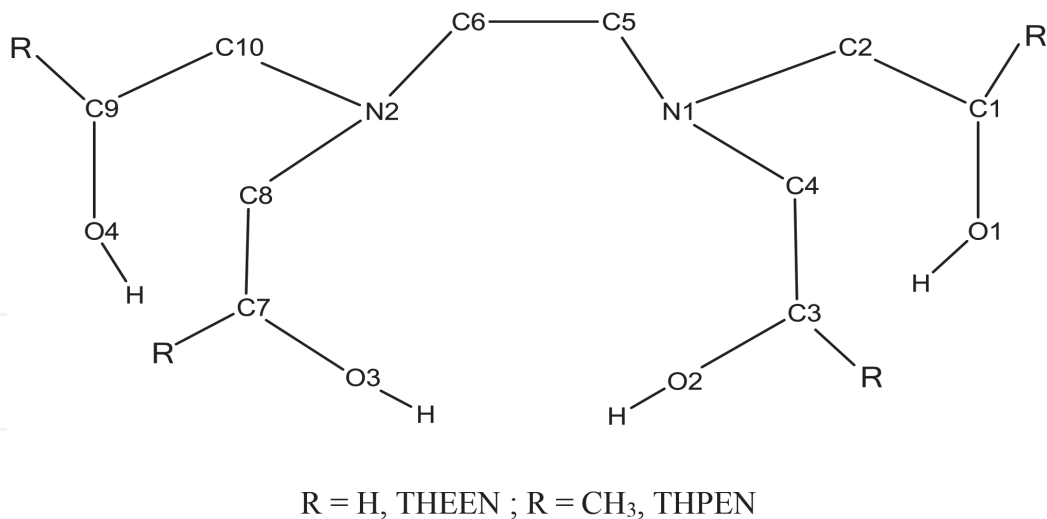
**Figure S4.** Plot showing the deviations of theoretical and experimental (a) bond lengths (Å) and (b) bond angles (°) for the complex (4) (c) (HOMO-LUMO) of the complex (4) with energy gap.



**Figure S5.** Plot showing the deviations of theoretical and experimental (a) bond lengths (Å) and (b) bond angles (°) for the complex (5) (c) (HOMO-LUMO) of the complex (5) with energy gap.

**Figure S6.**

Plot showing the deviations of theoretical and experimental (a) bond lengths (Å) and (b) bond angles (°) for the complex (6) (c) (HOMO-LUMO) of the complex (6) with energy gap.

**Figure S7.**

R = H, THENN; R = CH<sub>3</sub>, THPEN.

Bond distances (Å)	Theoretical	Experimental	Dev.	Bond angles (°)	Theoretical	Experimental	Dev.
Complex (1)							
Ca-N1	2.600	2.600	0.000	N1-Ca-N1A	71.54	71.60	0.06
Ca-O1	2.387	2.388	0.001	N1-Ca-O2A	81.41	65.52	15.89
Ca-O2	2.495	2.496	0.001	N1-Ca-O1W	119.08	119.09	0.01

Bond distances (Å)	Theoretical	Experimental	Dev.	Bond angles (°)	Theoretical	Experimental	Dev.
Ca-O1W	2.439	2.439	0.000	N1-Ca-O1WA	143.89	143.89	0.00
				O1-Ca-O2	102.93	102.95	0.02
				O1-Ca-N1	67.80	67.79	0.01
				O1-Ca-O1W	79.82	79.85	0.03
				O1-Ca-N1A	132.22	132.22	0.00
				O1-Ca-O2A	84.37	84.36	0.01
				O1-Ca-O1A	159.11	159.10	0.01
				O1-Ca-O1WA	83.52	83.54	0.02
				O2-Ca-N1	65.50	65.52	0.02
				O2-Ca-O1W	74.11	74.10	0.01
				O2-Ca-N1A	81.42	81.40	0.02
				O2-Ca-O2A	139.33	139.89	0.56
				O2A-Ca-O1W	145.88	145.90	0.02
Complex (2)							
Ca-O1	2.45	2.41	0.04	O1-Ca-O2	94.43	102.08	7.65
Ca-O2	2.45	2.38	0.07	O1-Ca-O3	172.00	175.21	3.21
Ca-O3	2.41	2.48	0.07	O1-Ca-O4	85.56	74.35	11.21
Ca-O4	2.41	2.37	0.04	O1-Ca-O12	107.80	104.18	3.62
Ca-O12	2.31	2.30	0.01	O1-Ca-O13	61.91	64.85	2.94
Ca-O13	2.47	2.73	0.26	O1-Ca-N1	65.93	68.50	2.57
Ca-N1	2.74	2.59	0.15	O1-Ca-N2	104.33	115.49	11.16
Ca-N2	2.82	2.65	0.17	O2-Ca-O3	90.99	79.27	11.72
				O2-Ca-O4	180.00	168.65	11.35
				O2-Ca-O12	108.06	107.20	0.86
				O2-Ca-O13	61.38	69.92	8.54
				O2-Ca-N1	64.20	68.43	4.23
				O2-Ca-N2	114.39	105.72	8.67
				O3-Ca-O4	89.01	105.24	16.23
				O3-Ca-O12	75.95	71.06	4.89
				O3-Ca-O13	126.03	110.69	15.34
				O3-Ca-N1	111.54	116.18	4.64
				O3-Ca-N2	67.97	68.26	0.29
				O4-Ca-O12	71.93	84.20	12.27
				O4-Ca-O13	118.62	116.91	1.71
				O4-Ca-N1	115.80	100.38	15.42
				O4-Ca-N2	65.61	67.36	1.75
				O12-Ca-O13	71.32	62.19	9.13
				O12-Ca-N1	168.56	169.55	0.99
				O12-Ca-N2	123.47	120.54	2.93
				O13-Ca-N1	97.26	107.46	10.2

Bond distances (Å)	Theoretical	Experimental	Dev.	Bond angles (°)	Theoretical	Experimental	Dev.
				O13-Ca-N2	163.73	175.60	11.87
				N1-Ca-N2	67.95	69.92	1.97
Complex (3)							
Ba-O1	2.720	2.720	0.000	O1-Ba-O2	86.95	87.00	0.05
Ba-O2	2.807	2.801	0.006	O1-Ba-O3	172.87	173.00	0.13
Ba-O3	2.753	2.750	0.003	O1-Ba-O4	88.55	88.50	0.05
Ba-O4	2.812	2.812	0.000	O1-Ba-O6	72.90	72.90	0.00
Ba-O5	2.681	2.683	0.002	O1-Ba-O12	61.79	61.80	0.01
Ba-O6	3.127	3.128	0.001	O1-Ba-O18	109.63	109.70	0.07
Ba-O12	2.728	2.729	0.001	O1-Ba-N1	58.12	58.10	0.02
Ba-O18	2.977	2.979	0.002	O1-Ba-N2	114.85	114.80	0.05
Ba-N1	3.038	3.038	0.000	O2-Ba-O4	129.37	129.40	0.03
Ba-N2	3.026	3.028	0.002	O2-Ba-O6	64.79	64.80	0.01
				O2-Ba-O18	161.62	160.60	0.02
				O2-Ba-N2	79.36	79.40	0.03
				O2-Ba-N1	57.03	57.12	0.05
				O3-Ba-O2	92.08	92.10	0.02
				O3-Ba-O4	86.61	86.70	0.09
				O3-Ba-O6	113.02	113.10	0.08
				O3-Ba-O18	72.70	72.80	0.10
				O3-Ba-N1	115.63	115.60	0.03
				O3-Ba-N2	58.06	58.20	0.14
				O4-Ba-O6	156.82	156.80	0.02
				O4-Ba-O18	63.13	63.20	0.07
				O4-Ba-N1	78.20	78.20	0.00
				O4-Ba-N2	57.43	57.40	0.03
				O5-Ba-O1	123.12	123.20	0.08
				O5-Ba-O2	85.94	85.90	0.04
				O5-Ba-O3	63.80	63.90	0.10
				O5-Ba-O4	135.92	135.90	0.02
				O5-Ba-O6	53.26	53.30	0.03
				O5-Ba-O12	84.0	84.00	0.00
				O5-Ba-O18	76.67	76.90	0.13
				O5-Ba-N1	142.90	142.90	0.00
				O5-Ba-N2	118.97	118.90	0.07
				O12-Ba-O2	133.15	133.20	0.05
				O12-Ba-O3	123.02	123.00	0.02
				O12-Ba-O4	86.45	86.40	0.05
				O12-Ba-O6	72.69	72.70	0.01
				O12-Ba-O18	54.05	54.00	0.05

Bond distances (Å)	Theoretical	Experimental	Dev.	Bond angles (°)	Theoretical	Experimental	Dev.
				O12-Ba-N1	117.95	117.96	0.01
				O12-Ba-N2	143.78	143.80	0.02
				O18-Ba-O6	109.54	109.60	0.06
				O18-Ba-N1	140.27	140.40	0.13
				O18-Ba-N2	101.49	101.50	0.01
				N2-Ba-N1	61.27	61.30	0.03
				N2-Ba-O6	143.21	143.20	0.01
				N1-Ba-O6	102.39	102.40	0.01
Complex (4)							
Na-N1	2.552	2.554	0.002	O1-Na-O2	99.56	99.50	0.06
Na-N2	2.565	2.566	0.001	O1-Na-O3	86.59	86.60	0.01
Na-O1	2.412	2.412	0.000	O1-Na-O4	174.34	174.30	0.04
Na-O2	2.393	2.393	0.000	O1-Na-O4A	90.18	90.23	0.05
Na-O3	2.505	2.505	0.000	O1-Na-N1	69.82	69.82	0.00
Na-O4	2.628	2.629	0.001	O1-Na-N2	109.13	109.10	0.03
Na-O4A	2.442	2.443	0.001	O2-Na-O3	164.10	164.13	0.03
Na-NaA	3.429	3.430	0.001	O2-Na-O4	78.26	78.31	0.05
				O2-Na-O4A	88.56	88.57	0.01
				O2-Na-N1	70.69	70.70	0.01
				O2-Na-N2	121.68	121.71	0.03
				O3-Na-O4	96.86	96.87	0.01
				O3-Na-N1	125.19	125.17	0.02
				O3-Na-N2	68.93	68.91	0.02
				O3-Na-O4A	76.69	76.72	0.03
				O4-Na-O4A	94.96	95.00	0.03
				O4-Na-N1	68.25	68.25	0.00
				O4-Na-N2	68.25	68.25	0.00
				N1-Na-N2	73.38	73.37	0.01
				N1-Na-O4A	147.48	147.51	0.03
				N2-Na-O4A	138.85	138.87	0.02
Complex(5)							
Sr-O1	2.617	2.618	0.001	O3-Sr-O2	151.28	158.70	7.42
Sr-O2	2.611	2.610	0.001	O3-Sr-O1	73.24	77.20	3.96
Sr-O3	2.506	2.505	0.001	O2-Sr-O1	113.98	114.30	0.32
Sr-O4	2.618	2.618	0.000	O3-Sr-O4	87.91	88.20	0.29
Sr-O1W	2.701	2.702	0.001	O2-Sr-O4	77.89	73.50	4.39
Sr-O2W	2.699	2.699	0.000	O1-Sr-O4	158.36	151.60	6.76
Sr-O2WA	2.726	2.699	0.000	O3-Sr-N1	102.34	113.60	11.26
Sr-N1	2.835	2.835	0.000	O4-Sr-N1	113.34	102.50	10.84
Sr-N2	2.849	2.849	0.000	O3-Sr-N2	61.38	64.40	3.02

Bond distances (Å)	Theoretical	Experimental	Dev.	Bond angles (°)	Theoretical	Experimental	Dev.
				O2-Sr-N2	89.92	97.10	7.18
				O1-Sr-N2	96.80	90.2	6.60
				O4-Sr-N2	64.13	61.60	2.53
				O3-Sr-O2W	106.07	106.40	0.33
				O2-Sr-O2W	70.58	77.10	6.52
				O1-Sr-O2W	129.35	140.50	11.15
				O4-Sr-O2W	70.80	67.90	2.90
				O2-Sr-O1W	79.52	65.40	14.12
				O1-Sr-O1W	65.11	79.80	14.69
				O4-Sr-O1W	136.42	127.40	9.02
				O3'-Sr-O1W	126.14	127.90	1.76
				O2W-Sr-O1W	70.75	71.00	0.25
				O2W-Sr-N2	128.11	128.40	0.29
				O1W-Sr-N2	152.06	152.40	0.34
				N1-Sr-N2	64.77	65.00	0.23
				O2W-Sr-N1	139.03	139.30	0.27
				O1W-Sr-N1	87.52	87.80	0.28
Complex (6)							
Ba-O1	2.736	2.738	0.002	O4-Ba-O1	162.70	162.90	0.20
Ba-O2	2.763	2.761	0.002	O4-Ba-O3	92.45	92.70	0.25
Ba-O3	2.756	2.757	0.001	O1-Ba-O3	79.69	80.00	0.31
Ba-O4	2.658	2.657	0.001	O4-Ba-O2	84.25	84.60	0.35
Ba-O1W	2.880	2.880	0.000	O1-Ba-O2	94.22	94.50	0.28
Ba-O2W	2.988	2.990	- 0.002	O3-Ba-O2	148.19	148.40	0.21
Ba-N1	3.009	3.002	0.007	O4-Ba-N1	107.19	107.50	0.31
Ba-N2	3.010	3.004	0.006	O1-Ba-N1	58.19	58.40	0.21
				O3-Ba-N1	91.90	92.00	0.01
				O2-Ba-N1	59.43	59.60	0.17
				O4-Ba-N2	59.95	61.10	1.15
				O1-Ba-N2	103.03	103.20	0.17
				O3-Ba-N2	58.68	58.80	0.12
				O2-Ba-N2	93.2	93.40	0.20
				N1-Ba-N2	61.84	62.00	0.16
				O4-Ba-O1W	126.17	126.50	0.33
				O1-Ba-O1W	66.29	66.50	0.23
				O3-Ba-O1W	72.53	72.80	0.27
				O2-Ba-O1W	133.50	133.80	0.30
				O1-Ba-O2W	73.43	73.70	0.27
				O3-Ba-O2W	131.18	131.50	0.32

Bond distances (Å)	Theoretical	Experimental	Dev.	Bond angles (°)	Theoretical	Experimental	Dev.
				O2-Ba-O2W	74.74	75.00	0.26
				O2W-Ba-O1WA	59.36	59.50	0.14
				N1-Ba-O1WA	137.03	137.20	0.17
				N1-Ba-O1W	124.19	124.19	0.00
				N1-Ba-O2W	106.68	106.90	0.22
				N2-Ba-O1WA	123.73	124.00	0.27
				N2-Ba-O1W	131.21	131.50	0.29
				N2-Ba-O2W	166.91	167.00	0.10
				N2-Ba-O2WA	100.84	100.87	0.03

**Table S1.**

Comparison of selected experimental and calculated geometric parameters bond lengths (Å) and bond angles (°) for complexes (1–6).

## Author details

Rakesh Kumar<sup>1\*</sup> and Sangeeta Obrai<sup>2</sup>

1 Department of Chemistry, MCM DAV College, Kangra, Himachal Pradesh, India

2 Department of Chemistry, Dr. B.R. Ambedkar National Institute of Technology, Jalandhar, Punjab, India

\*Address all correspondence to: [rakesh\\_nitj@yahoo.co.in](mailto:rakesh_nitj@yahoo.co.in)

## IntechOpen

© 2020 The Author(s). Licensee IntechOpen. This chapter is distributed under the terms of the Creative Commons Attribution License (<http://creativecommons.org/licenses/by/3.0>), which permits unrestricted use, distribution, and reproduction in any medium, provided the original work is properly cited. 

## References

- [1] Lehn JM. Structure and bonding. Alkali Metal Complexes with Organic Ligands. In: Dunitz JD, Hemmrich P, Ibers JA, Jorgensen CK, Neilsen JB, Reinan D, Williams RJP, editors. Vol. 16, 7. New York: Springer-Verlag; 1973
- [2] Tümmler B, Maas G, Weber E, Wehner W, Vögtle F. Noncyclic crown-type polyethers, pyridinophane cryptands, and their alkali metal ion complexes: Synthesis, complex stability, and kinetics. *Journal of the American Chemical Society*. 1977;**99**:4688
- [3] Cram DJ, Cram JM. Design of complexes between synthetic hosts and organic guests. *Accounts of Chemical Research*. 1978;**11**:8
- [4] Cram DJ. Preorganization - from solvents to spherands. *Angewandte Chemie (International Ed. in English)*. 1986;**25**:1039
- [5] Poonia NS, Bajaj AV. Coordination chemistry of alkali and alkaline earth cations. *Chemical Reviews*. 1979;**79**:145
- [6] Bajaj AV, Poonia NS. Comprehensive coordination chemistry of alkali and alkaline earth cations with macrocyclic multidentates: Latest position. *Coordination Chemistry Reviews*. 1988;**87**:55
- [7] Vögtle F, Müller WM, Buhleier E, Weber W. Synthesis and selectivity of novel four armed noncyclic neutral ligands. *Chemische Berichte*. 1979; **112**:899
- [8] Vögtle F, Weber E. Multidentate acyclic neutral ligands and their complexation. *Angewandte Chemie (International Ed. in English)*. 1979; **18**:753
- [9] Vögtle F, Weber E. Crystalline 1: 1 alkali metal complexes of noncyclic neutral ligands. *Tetrahedron Letters*. 1975;**16**:2415
- [10] Hay BP, Rustad JR. Structural criteria for the rational design of selective ligands: Extension of the MM3 force field to aliphatic ether complexes of the alkali and alkaline earth cations. *Journal of the American Chemical Society*. 1994;**116**:6316
- [11] Wipff G, Weiner P, Kollman P. A molecular-mechanics study of 18-crown-6 and its alkali complexes: An analysis of structural flexibility, ligand specificity, and the macrocyclic effect. *Journal of the American Chemical Society*. 1982;**104**:3249
- [12] Grootenhuis PDJ, Kollman PA. Molecular mechanics and dynamics studies of crown ether-cation interactions: Free energy calculations on the cation selectivity of dibenzo-18-crown-6 and dibenzo-30-crown-10. *Journal of the American Chemical Society*. 1989;**111**:2152
- [13] Pretsch E, Badertscher M, Welti M, Maruizumi T, Morf WE, Simon W. Design features of ionophores for ion selective electrodes. *Pure and Applied Chemistry*. 1988;**60**:567
- [14] Badertscher M, Welti M, Pretsch E, Maruizumi T, Ha T-K, Simon W. Combined application of pair potentials and the MM2 force field for the modeling of ionophores. *Journal of Computational Chemistry*. 1990;**11**:819
- [15] Varnek AA, Glebov AS, Petrukhin OM, Kolycheva NV, Ozerov RP. Selectivity of reactions of 18-crown-6 complexation with alkali-metals. *Koordinatsionnaya Khimiya (Russian Journal of Coordination Chemistry)*. 1989;**15**:600
- [16] Burns JH, Kessler RM. Structural and molecular mechanics studies of bis(dibutylphosphato)aquastrontium-18crown-6 and analogues

alkaline-earth-metal complexes.  
*Inorganic Chemistry*. 1987;**26**:1370

[17] Wipff G, Kollman P. Molecular mechanical calculations on a macrocyclic receptor: The 222 cryptand and its alkali complexes. *Nouveau Journal de Chimie*. 1985;**9**:457

[18] Damu KV, Hancock RD, Wade PW, Boeyens JCA, Billing DG, Dobson SM. Control of metal-ion size-based selectivity through the structure of the oxygen-donor pendant groups on lariat ethers. A crystallographic and thermodynamic study. *Journal of the Chemical Society, Dalton Transactions*. 1991:293

[19] Kollman P, Wipff G, Singh UC. Molecular mechanical studies of inclusion of alkali cations into anisole spherands. *Journal of the American Chemical Society*. 1985;**107**:2212

[20] Maye PV, Venanzi CA. Host-guest preorganization and complementarity: A molecular mechanics and molecular dynamics study of cation complexes of a cyclic urea-anisole spherand. *Journal of Computational Chemistry*. 1991;**12**:994

[21] Lifson S, Felder CS, Shanzer A. Computational design of polylactone macrocyclic ionophores. *Journal of the American Chemical Society*. 1983;**105**:3866

[22] Lifson S, Felder CS, Shanzer A. Design, synthesis, and conformation of ion carriers. *Bopolymers*. 1983;**22**:409

[23] Lifson S, Felder CS, Shanzer A. Internal and external alkali ion complexes of enniatin B: An empirical force field analysis. *Biochemistry*. 1984;**23**:2577

[24] Lifson S, Felder CS, Shanzer A. Enniatin B and valinomycin as ion carriers: An empirical force field analysis. *Journal of Biomolecular Structure & Dynamics*. 1984;**2**:641

[25] Kumar R, Obrai S, Kaur A, Hundal G, Meehnian H, Jana AK. Synthesis, crystal structure determination and antimicrobial studies of copper(II) picrate complexes with N, N, N'''-tetrakis(2-hydroxyethyl/propyl) ethylenediamine and tris(2-hydroxyethyl)amine. *Polyhedron*. 2013;**56**:55

[26] Kumar R, Obrai S, Kaur A, Hundal MS, Meehnian H, Jana AK. Synthesis, crystal structure investigation, DFT analyses and antimicrobial studies of silver(I) complexes with N, N, N'''-tetrakis(2-hydroxyethyl/propyl) ethylenediamine and tris(2-hydroxyethyl)amine. *New Journal of Chemistry*. 2014;**38**:1186

[27] Kumar R, Obrai S, Jassal AK, Hundal MS. Supramolecular architectures of N, N,N'',N'''-tetrakis-(2-hydroxyethyl) ethylenediamine and tris(2-hydroxyethyl)amine with La(III) picrate. *RSC Advances*. 2014;**4**:59248

[28] Akhtar MN, Harrison WTA, Shahid M, Khan IU, Ejaz JI. Synthesis, crystal structure and biological activity of a cobalt(II) complex of N,N,N''-tetrakis(2-hydroxypropyl) ethylenediamine. *Transition Metal Chemistry*. 2016;**41**: 325-330

[29] Frisch MJ, Trucks GW, Schlegel HB, Scuseria GE, Robb MA, Cheeseman JR, et al. *Gaussian 03, (Revision B.04)*. Wallingford, Connecticut: Gaussian, Inc.; 2004

[30] Becke AD. Density-functional thermochemistry. III. The role of exact exchange. *The Journal of Chemical Physics*. 1993;**98**:5648

[31] Lee C, Yang W, Parr RG. Development of the Colle-Salvetti correlation-energy formula into a functional of the electron density. *Physical Review B*. 1988;**37**:785

[32] Paterson GA, Al-Laham MA. A complete basis set model chemistry. II.

Open-shell systems and the total energies of the first-row atoms. The Journal of Chemical Physics. 1991;**94**:6081

[33] Hay PJ, Wadt WR. Ab initio effective core potentials for molecular calculations. Potentials for the transition metal atoms Sc to Hg. The Journal of Chemical Physics. 1985;**82**:270

[34] Wadt WR, Hay PJ. Ab initio effective core potentials for molecular calculations. Potentials for main group elements Na to Bi. The Journal of Chemical Physics. 1985;**82**:284

[35] Hundal G, Hundal MS, Obrai S, Poonia NS, Kumar S. Metal complexes of tetrapodal ligands: synthesis, spectroscopic and thermal studies, and X-ray crystal structure studies of Na(I), Ca(II), Sr(II), and Ba(II) complexes of tetrapodal ligands N,N,N',N'-tetrakis(2-hydroxypropyl)ethylenediamine and N,N,N',N'-tetrakis(2-hydroxyethyl)ethylenediamine. Inorganic Chemistry. 2002;**41**:2077

[36] Mariappan G, Sundaraganesan N. Spectral and structural studies of the anti-cancer drug Flutamide by density functional theoretical method. Spectrochimica Acta Part A. 2014; **117**:604

[37] Fleming I. Frontier Orbitals and Organic Chemical Reactions. New York: John Wiley and Sons; 1976

[38] Balachandran V, Lalitha S, Rajeswari S, Rastogi VK. Theoretical investigations on the molecular structure, vibrational spectra, thermodynamics, HOMO-LUMO, NBO analyses and paramagnetic susceptibility properties of p-(p-hydroxyphenoxy)benzoic acid. Spectrochimica Acta Part A. 2014; **121**:575

[39] Raif K, Sinem O, Azizoglu A. Experimental and computational study

on [2,6-bis(3,5-dimethyl-N-pyrazolyl)pyridine]-(dithiocyanato)mercury(II). Polyhedron. 2007;**26**:5069

[40] Uesugi Y, Mizuno M, Shimojima A, Takahashi H. Resonance Raman and ab initio MO calculation studies of the structures and vibrational assignments of the T1 state and the anion radical of coumarin and its isotopically substituted analogues. The Journal of Physical Chemistry. 1997;**101**:268